



ELSEVIER

Available online at www.sciencedirect.com

SCIENCE @ DIRECT®

Journal of Sound and Vibration 285 (2005) 571–583

JOURNAL OF
SOUND AND
VIBRATION

www.elsevier.com/locate/jsvi

Computation of the rms state variables and control forces in a half-car model with preview active suspension using spectral decomposition methods

A.G. Thompson^a, B.R. Davis^{b,*}

^a*School of Mechanical Engineering, University of Adelaide, S.A., 5005, Australia*

^b*School of Electrical and Electronic Engineering, University of Adelaide, S.A., 5005, Australia*

Received 10 June 2003; received in revised form 27 January 2004; accepted 26 August 2004

Available online 23 November 2004

Abstract

Spectral decomposition methods are applied to compute accurately the rms values for the control forces, suspension strokes and tyre deflection at front and rear in a half-car model with preview. The vehicle model is assumed to be fitted with active suspension and travelling at constant speed on a random road and the control is assumed to be optimal.

© 2004 Elsevier Ltd. All rights reserved.

1. Introduction

Explicit formulae for the computation of rms values for control force, suspension stroke and tyre deflection in the case of a quarter-car model with an optimally controlled active suspension without preview are given in a technical note by Thompson and Davis [1]. The computations only require the solution of Riccati and Lyapunov matrix equations. The rms values determined depend on the vehicle speed and road roughness and a simple formula is obtained for the performance index. Subsequently an expression for the performance index of a quarter-car model

*Corresponding author. Tel.: +61 8 8303 5667; fax: +61 8 8303 4360.

E-mail address: davis@eleceng.adelaide.edu.au (B.R. Davis).

with preview was obtained by Thompson and Pearce [2], and this was later extended to the determination of the performance index for a half-car model with preview active suspension [3].

In a further development [4], the rms values for force, stroke and deflection in a quarter-car model with preview have been shown to be obtainable analytically through the solution of a Lyapunov matrix equation using Matlab computer programs. Very accurate results were obtained by this method except in the case of low vehicle speed ($V < 2.5$ m/s). The determination of the rms values in the case of a half-car model with preview is accomplished by direct matrix manipulations employing a composite state 16-vector and corresponding composite state equation [5]. The solution in this case while analytically elegant and compact also gives very accurate rms values at all except very low vehicle speeds ($V < 3$ m/s approx.)

The method which we introduce in the following yields accurate rms values at all speeds and does not require the solution of Lyapunov type matrix equations or the manipulation of 16×16 composite matrices. The method is based on the spectral decomposition of a matrix as applied to the case of the half-car model with preview.

2. Road input and response

For a variety of roads the power spectral density of the random disturbance at a road to tyre contact point is approximated by

$$\Phi(\omega) = \frac{cV}{\omega^2} \text{ m}^2\text{s/rad} \quad (1)$$

where c is the road roughness constant and V is the velocity of travel. This equation represents integrated white noise which is useful as a theoretical input signal due to the fact that the mean-square value of any output signal of interest is simply related to the integral-square value of the corresponding response to a unit step in the road profile traversed at the same speed. For example, the mean-square value of the control force at either the front or the rear suspension due to the random road excitation is

$$\langle u_r^2(t) \rangle = 2\pi cV \int_0^\infty u_s^2(t) dt \quad (2)$$

where $u_s(t)$ is the control force at the same position due to a unit step in the road profile [1,5]. Whether the 2π factor is included or not depends on how the power spectral density is defined [6]. It is to be noted that for the half-car model where the same input is applied to the front tyre contact point and, after a speed-dependent interval T_d , at the rear tyre contact point, the output $y(t)$ at any point of the system is by superposition of the sum of the outputs due to each of these inputs acting separately. In applying (2) therefore, to model the half-car model, both $u_r(t)$ and $u_s(t)$ are taken as the values of the control forces at the same position and similarly for any other variables of interest.

A convenience of (1) is that all roads, rough or smooth, may be represented by a single parameter c . Comprehensive trade-off performance plots for different vehicle speeds and road conditions with rms values for suspension stroke, tyre deflection, support point accelerations, etc.

are presented by Hrovat [7,8] employing data obtained through digital simulation. Our object here, of course, is to derive this data through direct matrix computations.

3. The state equations

In the model shown in Fig. 1, V is the vehicle speed and P_s is the sensor preview distance. The road input $x_r(t) = U(t)$ is a unit step function which is detected by the preview sensor at the initial time $t = 0$. The ensuing disturbance inputs at the tyre contact points are then represented by

$$w_1 = x_a(t) = U(t - T_1), \quad w_3 = x_b(t) = U(t - T_2),$$

where the preview time is $T_1 = P_s/V$, the delay time is $T_d = L/V$ and $T_2 = T_1 + T_d$. The wheelbase is $L = a + b$, where a and b are the distances from the centre of gravity of the body from the front and rear support points, respectively.

The car is divided longitudinally by a vertical plane so that M is half the total body mass and J is half the pitch moment of inertia about a transverse axis through the centre of gravity. The front and rear unsprung masses M_1 and M_3 each correspond to a single wheel, while S_1 and S_3 represent the tyre spring rates. In considering the vertical motions, the control forces u_1 and u_3 are assumed to be applied between the wheels and the body at the front and rear, respectively. The vertical displacements x_1 – x_4 are measured from equilibrium on a level road and together with the corresponding velocities x_5 to x_8 form a set of eight state variables which are all zero initially.

The state equations for the half-car model may be derived as

$$\begin{aligned} \dot{x}_1 &= x_5, & \dot{x}_2 &= x_6, & \dot{x}_3 &= x_7, & \dot{x}_4 &= x_8, \\ \dot{x}_5 &= S_1(x_a - x_1)/M_1 - u_1/M_1, \\ \dot{x}_6 &= \alpha u_1 + \beta u_3, \end{aligned}$$

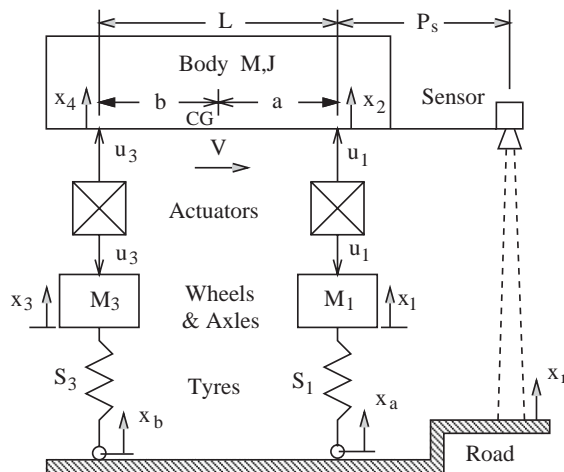


Fig. 1. Half-car model with preview encountering a unit step road input.

$$\begin{aligned}\dot{x}_7 &= S_3(x_b - x_3)/M_3 - u_3/M_3, \\ \dot{x}_8 &= \beta u_1 + \gamma u_3, \\ \alpha &= 1/M + a^2/J, \quad \beta = 1/M - ab/J, \quad \gamma = 1/M + b^2/J.\end{aligned}$$

The performance index is defined as the infinite integral

$$\begin{aligned}\Pi &= \int_0^\infty [\rho_1 u_1^2 + \rho_3 u_3^2 + q_1(x_1 - x_a)^2 \\ &\quad + q_2(x_1 - x_2)^2 + q_3(x_3 - x_b)^2 + q_4(x_3 - x_4)^2] dt.\end{aligned}\quad (3)$$

With the above notation, the state vector $\mathbf{x} = [x_1 \ x_2 \ x_3 \ x_4 \ x_5 \ x_6 \ x_7 \ x_8]'$, the control force vector $\mathbf{u} = [u_1 \ u_3]'$, and the disturbance input vector $\mathbf{w} = [w_1 \ w_3]' = [x_a \ x_b]'$. A transformation to relative displacements may be achieved by defining new state variables

$$\begin{aligned}z_1 &= x_1 - x_a, & z_5 &= x_3 - x_b, \\ z_2 &= x_2 - x_1, & z_6 &= x_4 - x_3, \\ z_3 &= x_5, & z_7 &= x_7, \\ z_4 &= x_6, & z_8 &= x_8.\end{aligned}$$

The new state vector $\mathbf{z} = [z_1 \ z_2 \ z_3 \ z_4 \ z_5 \ z_6 \ z_7 \ z_8]'$ and the matrix transformation equation is

$$\mathbf{z} = \mathbf{C}\mathbf{x} + \mathbf{D}\mathbf{w},$$

where \mathbf{C} is an (8×8) matrix and \mathbf{D} is an (8×2) matrix as given in [3]. The transformed state equations are then

$$\begin{aligned}\dot{z}_1 &= z_3 - \dot{x}_a, & \dot{z}_5 &= x_7 - \dot{x}_b, \\ \dot{z}_2 &= z_4 - z_3, & \dot{z}_6 &= z_8 - z_7, \\ \dot{z}_3 &= -(S_1 z_1 + u_1)/M_1, & \dot{z}_7 &= -(S_3 z_5 + u_3)/M_3, \\ \dot{z}_4 &= \alpha u_1 + \beta u_3, & \dot{z}_8 &= \beta u_1 + \gamma u_3.\end{aligned}$$

In matrix form we therefore have

$$\dot{\mathbf{z}} = \mathbf{A}\mathbf{z} + \mathbf{B}\mathbf{u} + \mathbf{D}\dot{\mathbf{w}},$$

where \mathbf{A} is (8×8) and \mathbf{B} is (8×2) as also given in [3] and

$$\dot{\mathbf{w}} = [\dot{x}_a \ \dot{x}_b]' = [\delta(t - T_1) \ \delta(t - T_2)]'.$$

Partitioning the (8×2) matrix \mathbf{D} into columns $\mathbf{D} = [d_1 \ d_2]$ gives

$$d_1 = [-1 \ 0 \ 0 \ 0 \ 0 \ 0 \ 0 \ 0]' \quad \text{and} \quad d_2 = [0 \ 0 \ 0 \ 0 \ -1 \ 0 \ 0 \ 0]'$$

Hence,

$$\dot{\mathbf{z}} = \mathbf{A}\mathbf{z} + \mathbf{B}\mathbf{u} + d_1 \delta(t - T_1) + d_2 \delta(t - T_2).$$

The performance index (3) may be written as

$$\Pi = \int_0^\infty (\mathbf{z}'\mathbf{Q}\mathbf{z} + \mathbf{u}'\mathbf{R}\mathbf{u}) dt$$

by introducing the diagonal matrices

$$\begin{aligned} \mathbf{Q} &= \text{diag}[q_1 \ q_2 \ 0 \ 0 \ q_3 \ q_4 \ 0 \ 0], \\ \mathbf{R} &= \text{diag}[\rho_1 \ \rho_3]. \end{aligned}$$

Expressions for the control forces in the optimally controlled system are set up in the following section, based on the equations for a half-car model with preview as given in [3]. The feedback gains and feedforward components of the control forces are determined from the solution of the Riccati equation. In the practical case where the preview is turned off, however, the rms values may be computed for any arbitrarily given set of feedback gains using the spectral decomposition methods which follow.

4. The control equations

The optimal control forces u_1 and u_3 are components of the vector

$$\mathbf{u}(t) = -\mathbf{R}^{-1}\mathbf{B}'\{\mathbf{K}\mathbf{z}(t) + \mathbf{p}(t)\},$$

where $\mathbf{p}(t)$ is (8×1) and \mathbf{K} is the (8×8) positive definite symmetric matrix solution of the algebraic Riccati equation

$$\mathbf{A}'\mathbf{K} + \mathbf{K}\mathbf{A} - \mathbf{K}\mathbf{B}\mathbf{R}^{-1}\mathbf{B}'\mathbf{K} + \mathbf{Q} = 0.$$

The system equation then becomes

$$\dot{\mathbf{z}}(t) = \mathbf{W}\mathbf{z}(t) - \mathbf{B}\mathbf{R}^{-1}\mathbf{B}'\mathbf{p}(t) + \mathbf{D}\dot{\mathbf{w}}(t), \tag{4}$$

where \mathbf{W} is the optimal closed-loop system matrix

$$\mathbf{W} = \mathbf{A} - \mathbf{B}\mathbf{R}^{-1}\mathbf{B}'\mathbf{K}.$$

The preview function $\mathbf{p}(t)$ is the solution of the vector equation

$$\dot{\mathbf{p}} + \mathbf{W}'\mathbf{p} + \mathbf{K}\mathbf{D}\dot{\mathbf{w}} = 0. \tag{5}$$

The solution of (5) for $t \geq 0$ subject to the boundary condition $\mathbf{p}(\infty) = 0$ is given by the integral

$$\begin{aligned} \mathbf{p}(t) &= \int_t^\infty \exp(\mathbf{W}'(\tau - t))\mathbf{K}\mathbf{D}\dot{\mathbf{w}}(\tau) d\tau \\ &= e^{\mathbf{W}'(T_1-t)}\mathbf{K}d_1U(T_1 - t) + e^{\mathbf{W}'(T_2-t)}\mathbf{K}d_2U(T_2 - t), \end{aligned} \tag{6}$$

where $U(t)$ is the unit step function.

5. Solutions for the state vector

Eqs. (4) and (5) can be combined into a composite equation

$$\begin{bmatrix} \dot{\mathbf{z}} \\ \dot{\mathbf{p}} \end{bmatrix} = \begin{bmatrix} W & -BR^{-1}B' \\ 0 & -W' \end{bmatrix} \begin{bmatrix} \mathbf{z} \\ \mathbf{p} \end{bmatrix} + \begin{bmatrix} D \\ -KD \end{bmatrix} \dot{\mathbf{w}}.$$

The initial state is found from $\mathbf{z}(0) = 0$ and $\mathbf{p}(0)$ obtained from (6).

To find the rms values in the next section we need to convert the system to a diagonal form.

The eigenvalue equation in terms of (8×8) submatrices is given by

$$\begin{bmatrix} W & -BR^{-1}B' \\ 0 & -W' \end{bmatrix} \begin{bmatrix} V_{11} & V_{12} \\ 0 & V_{22} \end{bmatrix} = \begin{bmatrix} V_{11} & V_{12} \\ 0 & V_{22} \end{bmatrix} \begin{bmatrix} A & 0 \\ 0 & -A \end{bmatrix}$$

and since A is in general complex, then the eigenvector matrix is also complex.

Multiplying out these equations gives

$$W V_{11} = V_{11} A, \quad (7)$$

$$-W' V_{22} = -V_{22} A, \quad (8)$$

$$W V_{12} - BR^{-1}B' V_{22} = -V_{12} A. \quad (9)$$

Now (7) shows that V_{11} is the matrix of the right eigenvectors of W , and A is a diagonal matrix of the eigenvalues of W , which because the system is stable, all have negative real parts.

Similarly, (8) shows that V_{22} is a matrix of the right eigenvectors of W' . It is easily shown that if $U_{11} = V_{11}^{-1}$ then $V_{22} = U_{11}'$ is a solution.

Lastly, (9) is a Lyapunov type equation which can be solved for V_{12} . However, a more direct method is to proceed as follows.

Now since $U_{11} W V_{11} = A$, the *spectral decomposition* of the matrices W and W' are

$$W = V_{11} A V_{11}^{-1},$$

$$W' = V_{22} A V_{22}^{-1}.$$

Then (9) becomes

$$\begin{aligned} V_{11} A V_{11}^{-1} V_{12} + V_{12} A &= BR^{-1}B' V_{22}, \\ A F + F A &= G, \end{aligned}$$

where

$$F = V_{11}^{-1} V_{12},$$

$$G = V_{11}^{-1} BR^{-1}B' V_{22}.$$

The elements of F are easily found as

$$F_{ij} = \frac{G_{ij}}{\lambda_i + \lambda_j},$$

$$V_{12} = V_{11} F.$$

The inverse of the composite eigenvector matrix is

$$\begin{aligned} \begin{bmatrix} U_{11} & U_{12} \\ 0 & U_{22} \end{bmatrix} &= \begin{bmatrix} V_{11} & V_{12} \\ 0 & V_{22} \end{bmatrix}^{-1}, \\ U_{11} &= V_{11}^{-1}, \\ U_{22} &= V_{22}^{-1}, \\ U_{12} &= -U_{11} V_{12} U_{22}. \end{aligned}$$

We now define

$$\begin{bmatrix} \mathbf{y}_a \\ \mathbf{y}_b \end{bmatrix} = \begin{bmatrix} U_{11} & U_{12} \\ 0 & U_{22} \end{bmatrix} \begin{bmatrix} \mathbf{z} \\ \mathbf{p} \end{bmatrix}.$$

Using (4) and (5) gives

$$\begin{bmatrix} \dot{\mathbf{y}}_a \\ \dot{\mathbf{y}}_b \end{bmatrix} = \begin{bmatrix} \mathcal{A} & 0 \\ 0 & -\mathcal{A} \end{bmatrix} \begin{bmatrix} \mathbf{y}_a \\ \mathbf{y}_b \end{bmatrix} + \begin{bmatrix} U_{11} & U_{12} \\ 0 & U_{22} \end{bmatrix} \begin{bmatrix} D \\ -KD \end{bmatrix} \dot{\mathbf{w}}.$$

The solution to this equation is

$$\begin{bmatrix} \mathbf{y}_a(t) \\ \mathbf{y}_b(t) \end{bmatrix} = \begin{bmatrix} e^{At} & 0 \\ 0 & e^{-At} \end{bmatrix} \left\{ \begin{bmatrix} \mathbf{y}_{0a} \\ \mathbf{y}_{0b} \end{bmatrix} + \begin{bmatrix} \mathbf{y}_{1a} \\ \mathbf{y}_{1b} \end{bmatrix} U(t - T_1) + \begin{bmatrix} \mathbf{y}_{2a} \\ \mathbf{y}_{2b} \end{bmatrix} U(t - T_2) \right\},$$

where from (6) we have using $W' = V_{22} \mathcal{A} U_{22}$

$$\begin{aligned} \mathbf{p}(0) &= e^{W'T_1} Kd_1 + e^{W'T_2} Kd_2 \\ &= V_{22} e^{AT_1} U_{22} Kd_1 + V_{22} e^{AT_2} U_{22} Kd_2 \end{aligned}$$

and

$$\begin{aligned} \begin{bmatrix} \mathbf{y}_{0a} \\ \mathbf{y}_{0b} \end{bmatrix} &= \begin{bmatrix} U_{11} & U_{12} \\ 0 & U_{22} \end{bmatrix} \begin{bmatrix} 0 \\ \mathbf{p}(0) \end{bmatrix} = \begin{bmatrix} U_{12} V_{22} (e^{AT_1} U_{22} Kd_1 + e^{AT_2} U_{22} Kd_2) \\ e^{AT_1} U_{22} Kd_1 + e^{AT_2} U_{22} Kd_2 \end{bmatrix}, \\ \begin{bmatrix} \mathbf{y}_{1a} \\ \mathbf{y}_{1b} \end{bmatrix} &= \begin{bmatrix} e^{-AT_1} (U_{11} - U_{12} K) d_1 \\ -e^{AT_1} U_{22} Kd_1 \end{bmatrix}, \\ \begin{bmatrix} \mathbf{y}_{2a} \\ \mathbf{y}_{2b} \end{bmatrix} &= \begin{bmatrix} e^{-AT_2} (U_{11} - U_{12} K) d_2 \\ -e^{AT_2} U_{22} Kd_2 \end{bmatrix}. \end{aligned}$$

We see later that for numerical reasons it is also useful to define the following:

$$\begin{aligned}
 \begin{bmatrix} \hat{\mathbf{y}}_{0a} \\ \hat{\mathbf{y}}_{0b} \end{bmatrix} &= \begin{bmatrix} e^{AT_1} & 0 \\ 0 & e^{-AT_1} \end{bmatrix} \begin{bmatrix} \mathbf{y}_{0a} \\ \mathbf{y}_{0b} \end{bmatrix} \\
 &= \begin{bmatrix} e^{AT_1} U_{12} V_{22} (e^{AT_1} U_{22} K d_1 + e^{AT_2} U_{22} K d_2) \\ U_{22} K d_1 + e^{A(T_2-T_1)} U_{22} K d_2 \end{bmatrix}. \\
 \begin{bmatrix} \hat{\mathbf{y}}_{1a} \\ \hat{\mathbf{y}}_{1b} \end{bmatrix} &= \begin{bmatrix} e^{AT_1} & 0 \\ 0 & e^{-AT_1} \end{bmatrix} \begin{bmatrix} \mathbf{y}_{1a} \\ \mathbf{y}_{1b} \end{bmatrix} \\
 &= \begin{bmatrix} (U_{11} - U_{12} K) d_1 \\ -U_{22} K d_1 \end{bmatrix}. \\
 \begin{bmatrix} \hat{\mathbf{y}}_{2a} \\ \hat{\mathbf{y}}_{2b} \end{bmatrix} &= \begin{bmatrix} e^{AT_2} & 0 \\ 0 & e^{-AT_2} \end{bmatrix} \begin{bmatrix} \mathbf{y}_{2a} \\ \mathbf{y}_{2b} \end{bmatrix} \\
 &= \begin{bmatrix} (U_{11} - U_{12} K) d_2 \\ -U_{22} K d_2 \end{bmatrix}. \\
 \begin{bmatrix} \hat{\mathbf{y}}_{3a} \\ \hat{\mathbf{y}}_{3b} \end{bmatrix} &= \begin{bmatrix} e^{AT_2} & 0 \\ 0 & e^{-AT_2} \end{bmatrix} \left\{ \begin{bmatrix} \mathbf{y}_{0a} \\ \mathbf{y}_{0b} \end{bmatrix} + \begin{bmatrix} \mathbf{y}_{1a} \\ \mathbf{y}_{1b} \end{bmatrix} + \begin{bmatrix} \mathbf{y}_{2a} \\ \mathbf{y}_{2b} \end{bmatrix} \right\} \\
 &= \begin{bmatrix} e^{AT_2} (\mathbf{y}_{0a} + \mathbf{y}_{1a} + \mathbf{y}_{2a}) \\ 0 \end{bmatrix}.
 \end{aligned}$$

6. The rms values

Direct computation of the rms values for the control force, suspension stroke and tyre deflection in the case of a quarter-car model with non-preview active suspension is described in [2] where the method is based on the assumption that the power spectral density of the random disturbance input $x_r(t)$ is approximated by that of integrated white noise, $S_{rr}(\Omega) = c/\Omega^2$ m²s/rad.

We are now in a position to determine analytically the rms values for the components of \mathbf{z} and \mathbf{u} .

First, we compute the matrix

$$P_{yy} = \int_0^\infty \mathbf{y}(t) \mathbf{y}^\dagger(t) dt = \int_0^\infty \begin{bmatrix} \mathbf{y}_a(t) \\ \mathbf{y}_b(t) \end{bmatrix} [\mathbf{y}_a^\dagger(t) \mathbf{y}_b^\dagger(t)] dt,$$

where \dagger is the complex conjugate transpose.

The elements of P_{yy} are easily calculated as

$$[P_{yy}](i,j) = \int_0^\infty \mathbf{y}(i) \mathbf{y}^*(j) dt$$

$$\begin{aligned}
 &= \int_0^\infty e^{\lambda_i t} \{ \mathbf{y}_0(i) + \mathbf{y}_1(i)U(t - T_1) + \mathbf{y}_2(i)U(t - T_2) \} \\
 &\quad \times \{ \mathbf{y}_0^*(j) + \mathbf{y}_1^*(j)U(t - T_1) + \mathbf{y}_2^*(j)U(t - T_2) \} e^{\lambda_j^* t} dt \\
 &= -\frac{1}{\lambda_i + \lambda_j^*} (P_0 + P_1 + P_2), \\
 P_0 &= \mathbf{y}_0(i)\mathbf{y}_0^*(j), \\
 P_1 &= \hat{\mathbf{y}}_0(i)\hat{\mathbf{y}}_1^*(j) + \hat{\mathbf{y}}_1(i)\hat{\mathbf{y}}_0^*(j) + \hat{\mathbf{y}}_1(i)\hat{\mathbf{y}}_1^*(j), \\
 P_2 &= \hat{\mathbf{y}}_3(i)\hat{\mathbf{y}}_2^*(j) + \hat{\mathbf{y}}_2(i)\hat{\mathbf{y}}_3^*(j) - \hat{\mathbf{y}}_2(i)\hat{\mathbf{y}}_2^*(j).
 \end{aligned}$$

For the case where $\lambda_i + \lambda_j^* = 0$ the result is

$$[P_{yy}](i, j) = -(P_1 T_1 + P_2 T_2).$$

This formulation avoids the numerical problems associated with the exponentials of large quantities which can occur at low vehicle velocities as T_1 and T_2 become large.

Now

$$\begin{bmatrix} \mathbf{z} \\ \mathbf{p} \end{bmatrix} = \begin{bmatrix} V_{11} & V_{12} \\ 0 & V_{22} \end{bmatrix} \begin{bmatrix} \mathbf{y}_a \\ \mathbf{y}_b \end{bmatrix}$$

so

$$\begin{aligned}
 P_{zz} &= \int_0^\infty \mathbf{z} \mathbf{z}^\dagger dt \\
 &= [V_{11} \ V_{12}] P_{yy} \begin{bmatrix} V_{11}^\dagger \\ V_{12}^\dagger \end{bmatrix}.
 \end{aligned} \tag{10}$$

Also from the relation

$$\mathbf{u} = -R^{-1} B' [K \ I] \begin{bmatrix} \mathbf{z} \\ \mathbf{p} \end{bmatrix} = -R^{-1} B' L \begin{bmatrix} \mathbf{y}_a \\ \mathbf{y}_b \end{bmatrix}$$

$$L = [KV_{11} \ KV_{12} + V_{22}]$$

we obtain

$$\begin{aligned}
 P_{uu} &= \int_0^\infty \mathbf{u} \mathbf{u}^\dagger dt \\
 &= R^{-1} B' L P_{yy} L^\dagger B R^{-1}.
 \end{aligned} \tag{11}$$

The diagonal elements of P_{zz} and P_{uu} are the required integral-squared values which can be converted to mean-square values using (2). In contrast to other methods [4,5], the method does not become numerically ill-conditioned at low velocities.

If required, the performance index can also be computed from the mean-square values of the components of \mathbf{z} and \mathbf{u} .

If the matrix W has repeated eigenvalues, then in general the matrix A is not diagonal and the calculation of mean square values becomes much more complicated. This situation is extremely

unlikely to occur in practice and for the system considered the eigenvalues were $-26.303 \pm j78.270$, $-19.207 \pm j56.595$, $-7.8514 \pm j9.6223$ and $-6.4965 \pm j7.8652$, and were independent of the vehicle speed.

7. Example

For example purposes, the following numerical data is assumed:

$$\begin{aligned} M_1 &= 28.58 \text{ kg}, & M_3 &= 54.43 \text{ kg}, & M &= 505.1 \text{ kg}, \\ S_1 &= 155\,900 \text{ N/m}, & S_3 &= 155\,900 \text{ N/m}, & J &= 651.0 \text{ kgm}^2, \\ a &= 1.0978 \text{ m}, & b &= 1.4676 \text{ m}, & L &= 2.5654 \text{ m}, \\ c &= 10^{-5} \text{ m}, & q_1 &= q_5 = 10, & q_2 &= q_6 = 1, \\ P_s &= 1.0000 \text{ m}, & \rho_1 &= \rho_3 = 0.8 \times 10^{-9}. \end{aligned}$$

The performance index as computed from the integral-square values and their weighting factors for a unit step as well as the rms values computed from Eqs. (10) and (11) are shown in Table 1 for $V = 20 \text{ m/s}$ (72 km/h) and $V = 30 \text{ m/s}$ (108 km/h).

These results agree perfectly with results found by different methods [3,5]. Assuming a tyre compression at static equilibrium of $\delta_t = 2 \text{ cm}$ and an available wheel free travel of $\delta_w = 6.3 \text{ cm}$, the 3σ limits are not exceeded.

Figs. 2–4 show plots of computed rms tyre deflections, wheel clearances and control forces, respectively. The results have been calculated down to speeds of 0.1 m/s with no numerical problems. Generally all rms values tend to increase with speed and ultimately determine the maximum speed at which it is safe to travel.

Fig. 5 shows the performance index both with and without preview, and it can be seen that the use of preview reduces the performance index significantly.

It is to be noted that the computations are based on ideal active suspensions in which the desired actuator forces are achieved exactly. Practical systems may depart from this assumption as described in Refs. [9,10] or in other designs where additional compensating dynamics may be introduced.

Table 1

		$V = 20 \text{ m/s}$		$V = 30 \text{ m/s}$	
		$P_s = 1$	$P_s = 0$	$P_s = 1$	$P_s = 0$
Perf index	Π	0.41699	0.50355	0.46289	0.52956
Front	$\sigma(z_1)$	2.77 mm	4.10 mm	3.77 mm	5.02 mm
Front	$\sigma(z_2)$	9.71 mm	9.60 mm	13.4 mm	11.9 mm
Rear	$\sigma(z_5)$	3.18 mm	3.32 mm	4.04 mm	3.95 mm
Rear	$\sigma(z_6)$	6.32 mm	6.52 mm	8.17 mm	9.58 mm
Front	$\sigma(u_1)$	386.5 N	400.2 N	482.5 N	489.1 N
Rear	$\sigma(u_3)$	340.0 N	338.5 N	409.6 N	455.5 N

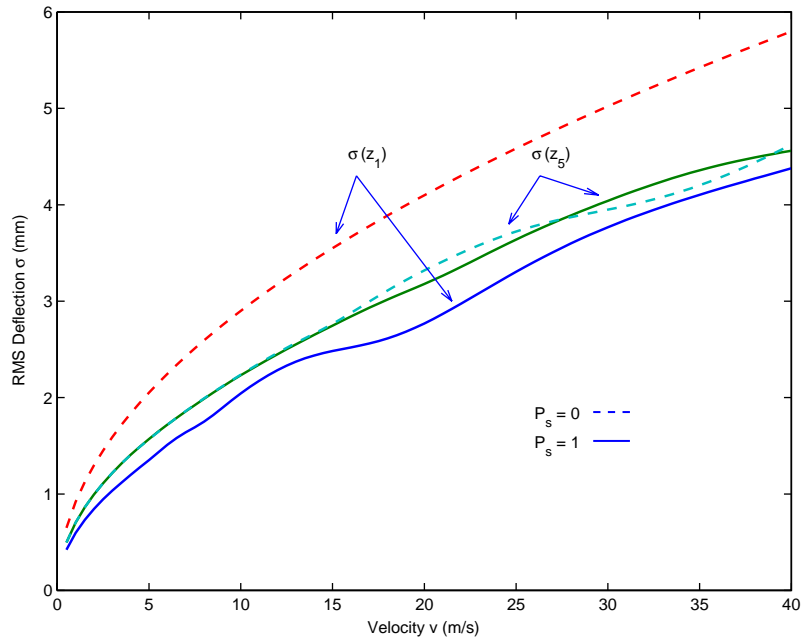


Fig. 2. RMS tyre deflections (front and rear).

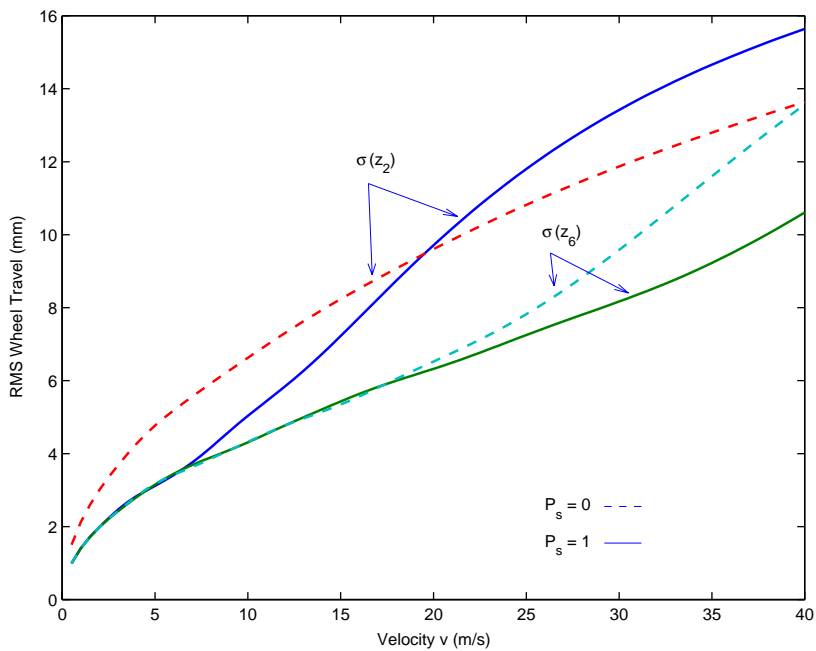


Fig. 3. RMS wheel travel variations (front and rear).

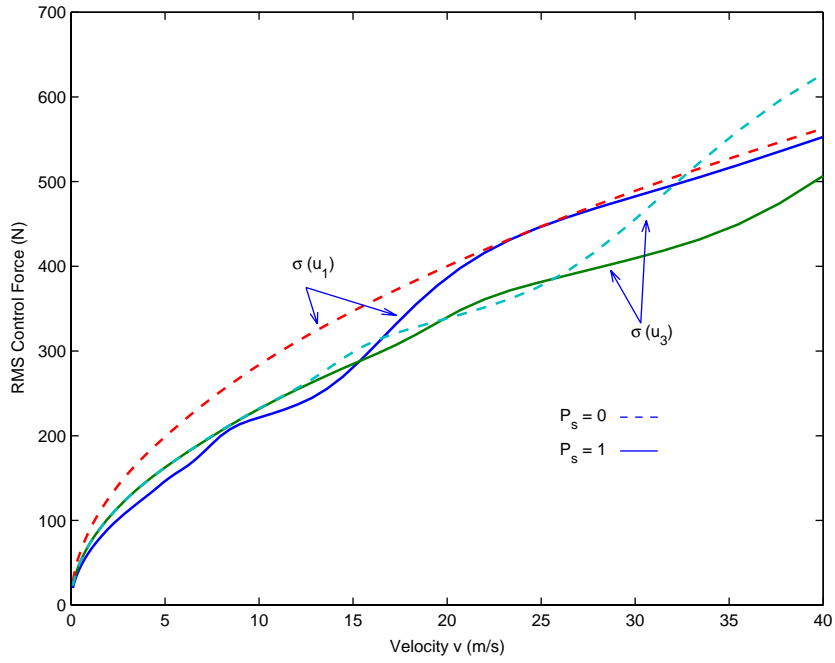


Fig. 4. RMS control forces (front and rear).

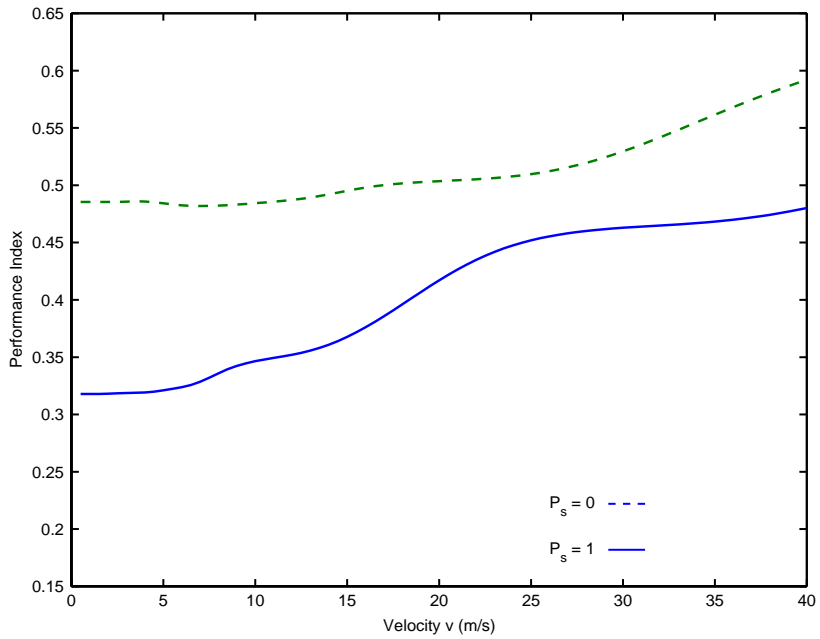


Fig. 5. Performance indices.

8. Conclusion

A technique for computing rms values and the performance index has been demonstrated. The method is more concise than simulation methods or previous methods of direct computation, and is easily implemented in Matlab^R.

References

- [1] A.G. Thompson, B.R. Davis, RMS values for control force, suspension stroke and tyre deflection in an active suspension, *Vehicle System Dynamics* 34 (2000) 143–150.
- [2] A.G. Thompson, C.E.M. Pearce, Performance index for preview active suspension applied to a quarter-car model, *Vehicle System Dynamics* 35 (2001) 55–66.
- [3] A.G. Thompson, C.E.M. Pearce, Direct computation of the performance index for an optimally controlled active suspension with preview applied to a half-car model, *Vehicle System Dynamics* 35 (2001) 121–137.
- [4] A.G. Thompson, C.E.M. Pearce, RMS values for force, stroke and tyre deflection in a quarter-car model active suspension, *Vehicle System Dynamics* 39 (2002) 57–75.
- [5] A.G. Thompson, B.R. Davis, RMS values of force, stroke and tyre deflection in a half-car model with preview controlled active suspension, *Vehicle System Dynamics* 39 (2003) 245–253.
- [6] B.R. Davis, A.G. Thompson, Power spectral density of road profiles, *Vehicle System Dynamics* 35 (2001) 409–415.
- [7] D. Hrovat, Survey of advanced suspension developments and related optimal control applications, *Automatica* 33 (1997) 1781–1817.
- [8] D. Hrovat, Optimal suspension performance for 2-D vehicle models, *Journal of Sound and Vibration* 146 (1) (1991) 93–110.
- [9] A.G. Thompson, P.M. Chaplin, Force control in active suspensions, *Vehicle System Dynamics* 25 (1996) 185–2002.
- [10] A.G. Thompson, B.R. Davis, Force control in electrohydraulic active suspensions revisited, *Vehicle System Dynamics* 35 (2001) 217–222.